15 Passive sampling of POP and PAH with virtual organisms in alpine environments

Karl-Werner Schramm[1,2], Marchela Pandelova[2]

15.1 Introduction

Virtual Organisms (VO) are defined as an artificial property-tool, and are reflecting exposomic processes in compartments of real organisms (Schramm et al. 2013). For instance, VO containing fat or proteins such as albumin can be employed to investigate the exposure of chemicals against such compartments which are common for many species in the kingdom of animals. The duration of VO exposure can be well defined and does not depend on the lifetime (Schramm et al. 2013). To estimate ambient concentrations VO are exposed and Performance Reference Compounds (PRC) are in use to estimate the sampling rate of air over time. Qualitatively the VO mainly sequestrated gas phase contaminants.

Exposomics is the study of the exposome and is related to genomics, metabonomics, lipidomics, transcriptomics, proteomics, and includes the study of exposures in the environment. Biomarkers of exposure and effect are targeted. The exposome of real organisms is defined as the measure of all the exposures of an individual in a lifetime and how those exposures relate to disease (CDC 2010). However, environmental exposomics has not been tackled so far although the definition can be extended to other organisms than humans. Further, molecular exposomics does not cover all exposomic aspects such as noise, radiation, pathogens but focuses only on the exposure of individuals to molecules or better chemicals and their effects within a lifetime. Individuals other than humans might have also advantages with respect to their observation due to their shorter lifetime or less transient exposure situation. If we look at the kingdom of molecules, resp. chemicals, the exposure to chemicals of transient behavior is difficult to quantify. In contrast, chemicals which are persistent and bioaccumulating are better and easier to investigate in exposomics due to their long lasting presence in compartments of individuals. In some cases the individuals even do not achieve equilibrium between their and environmental compartments during lifetime. Persistent Organic Pollutants (POP) once marketed are expected to remain in the environment and biota for a long time and might peak even years after their use in the following generations of individuals. Due to these POP properties the exposure can be accurately estimated. Thus molecular exposomics is reflecting time dependent exposure and effects of molecules with its intrinsic challenges and perspectives which are outlined besides for humans also for the environment and for VO of exposure sciences (Schramm et al. 2013).

15.2 Lipidome-VO

VO are artificially designed to simulate the specific biological compartment such as fat as a part of the lipidome of an organism. VO reflecting this fatty compartment and especially POP are accumulating to a large extend in fatty tissues as an important part of the long lasting storage compartment of persisting and very Persistent very Bioaccumulative Toxic compounds (vPvBT) of real organism's exposome. **V**O consists of Polyethylene (PE) lay-flat tubing enclosing a thin film of natural-like trioleine, a high molecular weight (MW = 885 g/mole) natural lipid. VO can develop a biofilm during exposure. Therefore stable isotope labelled **P**erformance **R**eference **C**ompounds (**PRC**) are added into the VO-triolein to compensate environmental conditions at different sampling locations such as turbidity, temperature, biofouling etc. during exposure. **PRC** losses are then used to calculate the air volume sampled by the VO and thus to calculate the ambient mean concentrations of the PBT.

Several **VO** are placed in stainless steel container or Stevenson Huts which are usually deployed in air 2–12 weeks.

[1] TUM, Wissenschaftszentrum Weihenstephan für Ernährung und Landnutzung, Department für Biowissenschaften, Weihenstephaner Steig 23, 85350 Freising, Germany, schramm@wzw.tum.de
[2] Helmholtz Zentrum München (GmbH), Molecular EXposomics (MEX), Ingolstädter Landstr.1, D-85764 Neuherberg, Germany, schramm@helmholtz-muenchen.de
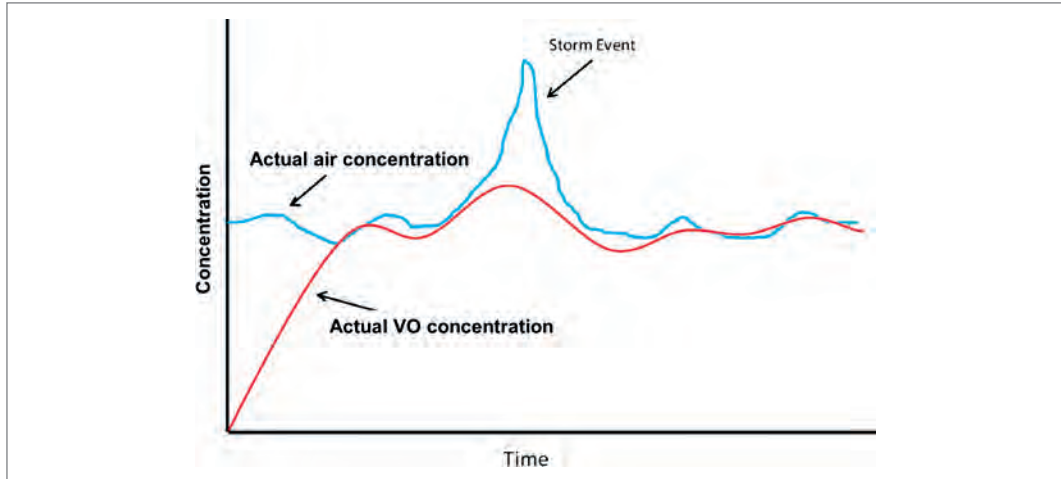
Fig. 1: Schematic representation of accumulation behavior for VO. The actual air concentration is integrated and averaged over time.
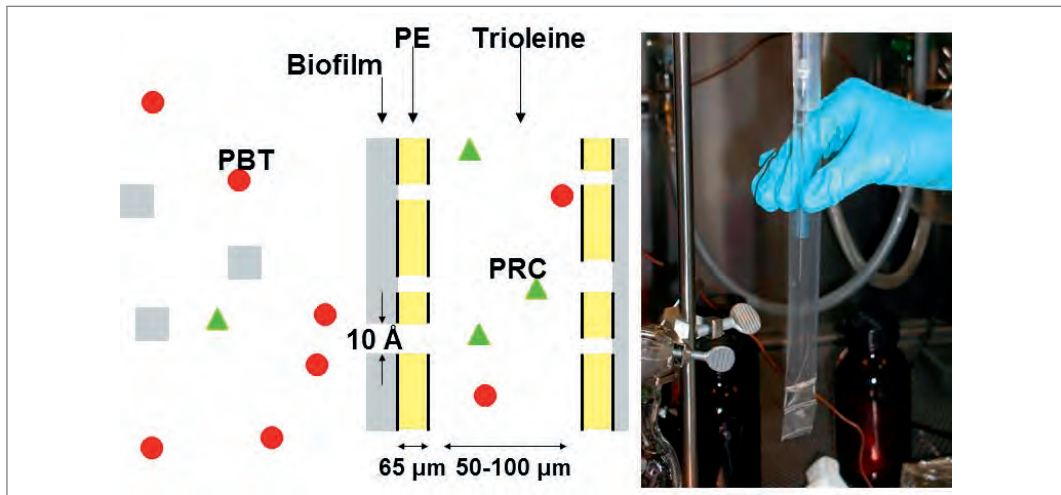
Fig. 2: Schematic representation of the uptake of the chemicals of interest and the elimination of the PRC into the environment as a measure of the air volume sampled by the VO (left). Right: picture of the lay-flat LPDE membrane filled with synthetic triolein similar to natural fat and representing the lipidome.

15.3 VO-theory

15.3.1 Kinetic Model

If the resistance to the mass transfer is controlled by the boundary layer, we can model the system considering the VO device as a one compartment as follows:
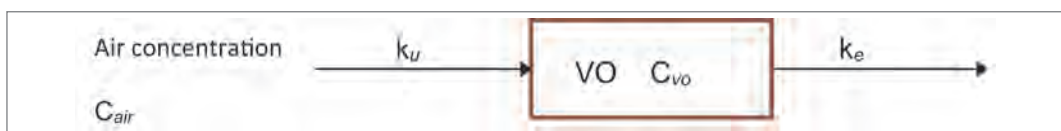
Fig. 3: Schematic representation of one compartment model for VO. Cair: compound concentration in air, k_u: uptake rate constant, C_{vo}: compound concentration within the VO, k_e: elimination rate constant.

Applying a mass balance in the VO compartment leads to:

$$\frac{\partial C_{vo}}{\partial t} = k_u C_{air} - k_e C_{vo}$$

Equation 1

Out of this mass balance, the relation between sampling time t, C_{vo} and C_{air} can be calculated. Regrouping and integrating equation 1 in a span of time t gives:

$$\frac{\partial C_{vo}}{(k_u C_{air} - k_e C_{vo})} = \partial t \Rightarrow \frac{-1}{k_e} \int_0^{c(t)} \frac{\partial C_{vo}}{\left(\frac{-k_u C_{air}}{k_e} + C_{vo}\right)} = \int_0^t \partial t \Rightarrow Ln\left|\frac{\frac{-k_u C_{air}}{k_e} + C_{vo}(t)}{\frac{-k_u C_{air}}{k_e}}\right| = -k_e t$$

Applying ex and regrouping: results in:

$$C_{vo}(t) = \frac{k_u C_{air}}{k_e}\left[1 - e^{-k_e t}\right] \Rightarrow C_{vo}(t) = K_{vo_a} C_{air}\left[1 - e^{-k_e t}\right] \qquad \text{Equation 2}$$

where K_{vo_a} is the VO-air partition coefficient $\left(K_{vo_a} = \frac{k_u}{k_e}\right)$.

When the VO is still in the linear stage, the amount of compound released from the VO to the air compartment is negligible, thus from equation 1 $k_e C_{vo} \to 0$

$$\Rightarrow \partial C_{vo}/\partial t \cong k_u C_{air} \qquad \text{Equation 3}$$

Integrating this approximation in a span of time t leads to:

$$C_{vo}(t) = k_u C_{air} t \quad \text{Linear uptake stage} \qquad \text{Equation 4}$$

When the VO has reached equilibrium conditions, such that the concentrations do not change anymore, equation 1 leads to:

$$\partial C_{vo}/\partial t = 0 \Rightarrow k_u C_{air} = k_e C_{vo} \qquad \text{Equation 5}$$

so the compound concentrations in the air and the VO are related through the uptake and elimination rate constants:

$$C_{air} = \frac{C_{vo} k_e}{k_u} = \frac{C_{vo}}{K_{vo_a}} \quad \text{Equilibrium conditions} \qquad \text{Equation 6}$$

15.3.2 Mass Transfer Coefficient Model

The mass transfer in the system can be described by means of mass transfer coefficients as follows:
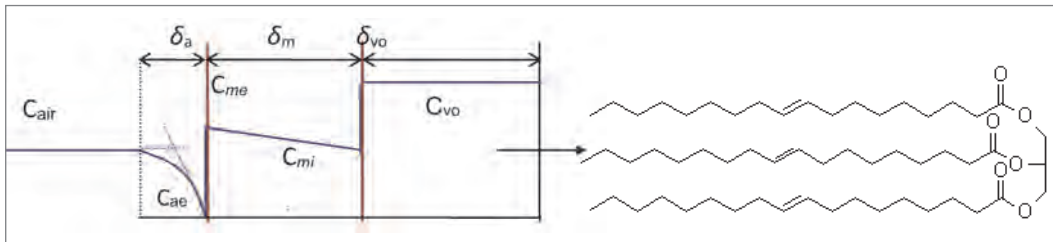
Fig. 4: Schematic overview of the concentration distribution air-VO. C_{air}: compound concentration in air, C_{ae}: compound concentration at the membrane outside boundary layer, C_{me}: compound concentration at the membrane inside boundary layer, C_{mi}: compound concentration at the membrane internal side, C_{vo}: compound concentration in VO, δ: effective thickness of each region and their associated subscripts.

Appling Fick's First law and assuming concentration homogeneity within the device, the flux F generated is

$$F = -DA\frac{\partial C}{\partial \delta}, \qquad \text{Equation 7}$$

where D is the diffusivity of the compound and A is the sectional area where the compound is transferred (membrane surface area). Substituting the mass transfer coefficients $k_m = D_m/\delta_m$ and $k_a = D_a/\delta_a$ in the equation:

$$F = k_m A_{vo}(C_{me} - C_{mi}) = k_a A_{vo}(C_{air} - C_{ae}) = V_{vo}\frac{\partial C_{vo}}{\partial t} \qquad \text{Equation 8}$$

Using the equilibrium partition coefficients defined as $K_{ms} = C_{mi}/C_{vo}$, $K_{ma} = C_{me}/C_{ae}$ and $K_{vo_a} = C_{vo}/C_{air}$ the equation is re-written as a function of the variables of interest C_{air} and C_{vo}, obtaining:

$$F = k_o A_{vo}(C_{air}K_{ma} - C_{vo}K_{ms}) = V_{vo}\frac{\partial C_{vo}}{\partial t} \qquad \text{Equation 9}$$

where k_o is the total mass transfer coefficient:

$$\frac{1}{k_o} = \frac{1}{k_m} + \frac{K_{ma}}{k_a} \qquad \text{Equation 10}$$

Assuming independence and additivity of the coefficients and regrouping and integrating the equation 3 we obtain:

$$C_{vo} = C_{air}\frac{K_{ma}}{K_{ms}}(1 - e^{-(k_o A_{vo}K_{ms}t/V_{vo})}) = C_{air}K_{vo_a}(1 - e^{-k_T t}) \qquad \text{Equation 11}$$

In this equation the overall uptake rate constant is defined as $k_T = k_o A_{VOms}K_{ms}/V_{vo}$ and K_{vo_a} is substituted by K_{ma}/K_{ms}.

Equation 1 and 5 describe the uptake stages depicted in Fig. 5. In short exposure periods (equation 5), for $t \rightarrow 0$ the limit of the exponential term tends to

$$\lim (1 - e^{-(k_o A_{vo}K_{ms}t/V_{vo})}) \rightarrow k_o A_{ov}K_{ms}t/V_{vo} \qquad \text{Equation 12}$$

Substituting this term in equation 5 a linear time-dependent function is obtained:

$$C = C_{air}K_{vo_a}k_o A_{vo}K_{ms}t/V_{vo} = C_{air}K_{ma}k_o A_{vo}t/V_{vo} \qquad \text{Equation 13}$$

In this linear stage, the uptake of compounds depends on the design of the device (volume and area) and the physical chemical properties of the chemical. The sampling rate R_s is defined as the volume of compound incorporated by the passive sampler per unit of time:

$$R_{vo} = K_{ma}k_o A_{vo} \qquad \text{Equation 14}$$

and substituting equation 14 in equation 13 :

$$C = C_{air}R_{vo}t/V_{vo} \Rightarrow R_{vo} = C_{vo}V_{vo}/C_{air}t \qquad \text{Equation 15}$$

In this way, in the linear uptake stage, the sampling rate of a compound can be calculated if the VO and air concentrations of the compound for a determined exposure time are known.
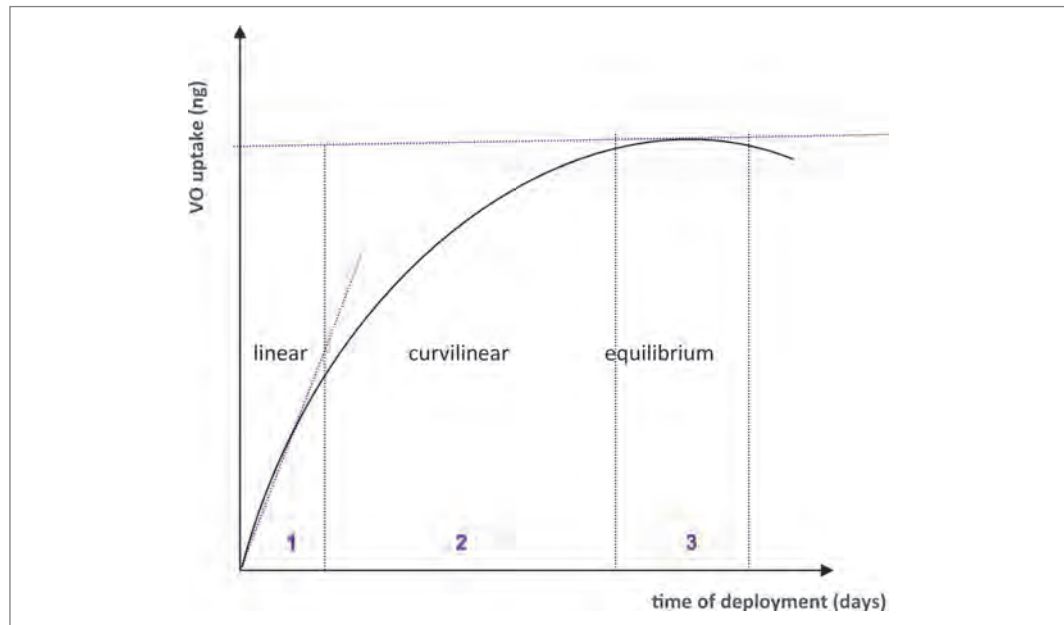
Fig. 5: Schematic overview of the concentration development in VO. If VO concentration is close to zero the accumulation proceeds in a pseudo-linear manner at times close to zero, followed by a curvilinear period and finally approaching constant concentrations at equilibrium with the air, provided that the air concentration remains nearly constant.

For the empirical calculation of sampling rates, $C_{vo}V_{vo}$ is equivalent to the amount of mass N_s sequestered in the VO. Substituting N_{vo} in the equation 15 leads to:

$$R_{vo} = N_{vo}/C_{air}t \qquad\qquad \text{Equation 16}$$

Once sampling rates for compounds have been established for a determined sampling design using equation 16, these sampling rates can be used to estimate the air concentrations of a compound, from the compound uptake into the VO and the time of deployment.

In devices deployed enough time to reach steady state conditions the exponential term of equation 11 tends to zero and thus:

$$C_{vo} = C_{air}K_{vo_a} \quad \text{equilibrium conditions} \qquad\qquad \text{Equation 17}$$

In the equilibrium stage the concentrations in air and VO_{fat} (triolein) are related exclusively through the $VO_{fat-air}$ partition coefficient K_{TA} (equation 29).

$$C_{vo_{fat}} = C_{air}K_{TA} \Rightarrow C_{air} = C_{vo_{fat}}/K_{TA} \qquad\qquad \text{Equation 18}$$

The equation 18 allows the calculation of the compound air concentration just knowing the K_{TA} value and the amount of chemical accumulated in the triolein under steady state conditions.

Note that the two models presented above can be related through the constants; elimination rate constant k_e in the kinetic model (equation 8) and overall uptake rate constant k_T in the mass transfer coefficient model (equation 11).

15.3.3 Performance Reference Compounds

Performance reference compounds (PRC) are non-interfering organic chemicals with medium to high affinity for triolein which are added to it before the membrane enclosure and distributed homogeneously in the lipid phase (Huckins et al., 2002). In preference, PRC have to be compounds not exhibited in the environment and due to this, 13C-PAH or 13C-PCB compounds are adequate. The purpose of these compounds is to compensate the effect of environmental variables at the different sampling sites. The theory is based on the assumption that the elimination rate (k_e) of PRC is related to the uptake rate (k_u) of the corresponding native compounds. The release of PRC follows an exponential decay with the exposure time:

$$\frac{\partial C_{PRC}}{\partial t} = -k_e C_{PRC} \Rightarrow \int_{C_{PRC_o}}^{C_{PRC}} \frac{\partial C_{PRC}}{C_{PRC}} = -k_e \int_0^t \partial t \Rightarrow C_{PRC} = C_{PRC_o}e^{-k_e t} \qquad \text{Equation 19}$$

The initial amount of PRC (C_{PRCo}) and the remaining amount after the exposure time (C_{PRC}) are known, such that the elimination rate can be calculated by regrouping the equation 19:

$$k_e = \frac{Ln\,(C_{PRC_o}/C_{PRC})}{t} \qquad\qquad \text{Equation 20}$$

The elimination rate constant ke is assumed to be also identical to the overall uptake rate constant k_T in the mass transfer coefficient model for the native and labelled compound leading to:

$$k_e = k_{ma}k_o A_{vo}/V_{vo}K_{vo_a} \Rightarrow k_e = R_{vo}/V_{vo}K_{vo_a} \Rightarrow k_e V_{vo}K_{vo_a} = R_{vo} \qquad \text{Equation 21}$$

where R_{vo} was substituted using the equation 14 from the mass transfer model. Equation 21 relates the sampling rate of the compound to the elimination rate obtained "in situ" for a determined compound with the PRC. In this way, the effects generated by differences in the exposure sampling conditions can be contemplated. Studies performed by Söderström and Bergqvist, (2004) with PRC demonstrated the influence of the wind speed in the sampling rate. As a consequence, the devices are sheltered in order to avoid differences due to wind effects affecting the turbulence and as a consequence the air-membrane boundary layer thickness (Ockenden et al., 2001). Additionally, the sheltering is also important to avoid photodegradation of compounds sensible to UV light. Some other environmental conditions, such as temperature, are also affecting the sampling rate. The use of PRC allows the R calculation regarding environmental conditions and even a posterior quantification of compounds in the environment.

15.3.4 VO data calculation

Sixteen 13C-PRC-PAH and three 13C-PRC-PCB retain in VO were used to calculate the sampling rates and polycyclic aromatic hydrocarbons (PAH), polychlorinated biphenyls (PCB) and organochlorine pesticides (OCP) water concentrations (Temoka et al., 2016). According to equation 21, the sampling rate of PRC R_{vo},PRC is estimated according to

$$R_{vo, PRC} = V_{vo}K_{VO_a}k_{e, PRC}$$

Equation 22

where V_{vo} is the VO volume (L), K_{VO_a}, the VO-air partition coefficient is the volume averaged partition coefficient (see below) of low density polyethylene (LPDE) and triolein ((mass/L)/(mass/L)) and $k_{e,PRC}$ is the elimination rate constant of PRCs per day (d–1). Thus, ke,PRC is given by:

$$k_{e,PRC} = -\frac{\ln(N_{t,PRC}/N_{0,PRC})}{t}$$

Equation 23

where $N_{0,PRC}$ is the related PRC fraction at the beginning of the exposure period and $N_{t,PRC}$ is the related PRC fraction after the exposure period (t). For compounds with very low $k_{e,PRC}$ values a minimal sampling rate $R_{vo_{min}}$ is further established and used as corrector value of R_{voPRC} (Temoka et al., 2017).

Subsequently, the obtained R_{vo} value was used to back-calculate the air concentrations (Ca) of the pollutants.

$$C_{air} = \frac{N}{V_{vo}K_{VO_a}(1 - \exp(-R_{vo.t}/V_{vo}K_{VO_a}))}$$

Equation 24

where N is the amount of analyte accumulated after a given exposure time.

However, PCB and OCP sampling rates (R_{vo}) were estimated on the base of resulted correlation coefficient $R^2 > 0.75$ regarding the relation between PRC-PAHs RsPRC and the exponential product of octanol-water partition coefficient log K_{ow} and molecular weight MW (g/mole).

$$R_{vo,analyte}(N) = a\,e^{b\,MW\,logKow}$$

Equation 25

where a and b are constants for a given exposure situation.

Triolein containing VO were utilized as passive samplers also for the three categories of substances PAH, PCB and OCP in air:

$$K_{V0-A} = \frac{K_{T.A}V_T + K_{LPDEA}V_{LPDE}}{V_T + V_{LPDE}}$$

Equation 26

where V_T is the volume of the triolein (cm^3), V_{LPDE} the volume of LPDE (cm^3), $K_{T.A}$ is the triolein-air partitioning coefficient (mass/m^3/ (mass/m^3) and K_{LPDEA} is the LPDE-air partitioning coefficient (mass/m^3/(mass/m^3).

$$\log K_{T.W} = \log K_{ow} + 0.105 \qquad \text{Chiou et al., 1985} \qquad \text{Equation 27}$$

and

$$\log K_{LPDEA} = 1.05 \log K_{ow} - 0.59 \qquad \text{Booij and Smedes, 2010} \qquad \text{Equation 28}$$

$$K_{TA} = \frac{K_{T.W}RT}{H}$$

Equation 29

$$K_{LPDEA} = \frac{K_{LPDEW}RT}{H}$$

Equation 30

where K_{ow} is the octanol-water partition coefficient, K_{TW} and K_{LPDEW} are the triolein- and LPDE-water partition coefficients, R is the ideal gas constant (8.314 Pa m^3 mol^{-1} K^{-1}), T is the absolute temperature (293 K) and H is the Henry's law constant of the chemicals (Pa m^3 mol^{-1}).

Finally, the gas-concentrations were estimated based on the performance of the reference compounds, which were used to estimate their sampling volume of the deployment period (Ockenden et al., 2001). The total concentrations were calculated on the basis of measured or estimated aerosol concentrations and by using $K_{aerosol-gas}$ (Mackay et al., 1986) partitioning followed by summing the gaseous and aerosol part per m^3.
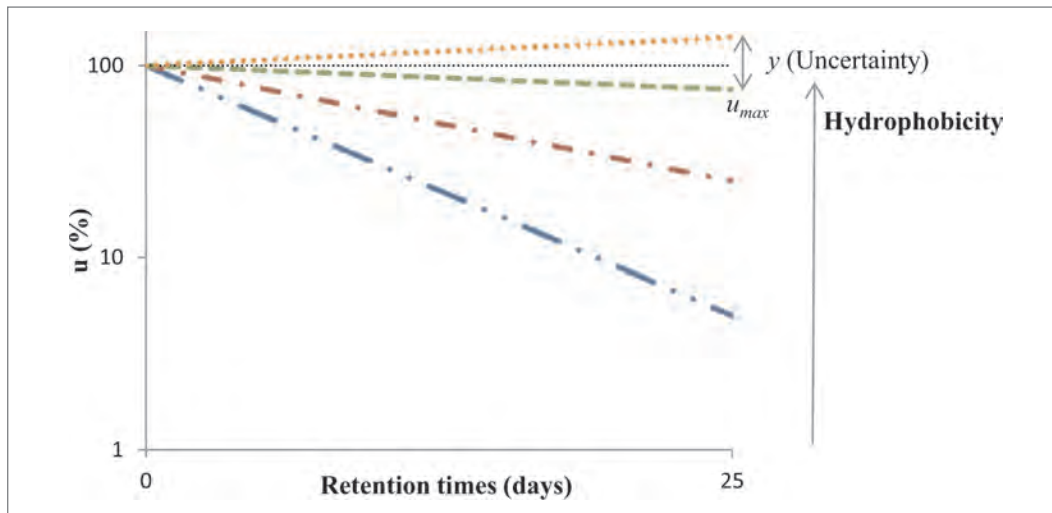
Fig. 6: Scheme representing uncertainty field of dissipated PRC values (u) during exposure times. u_{max} is the largest possible deviation from the average dissipation $\bar{u}$ of a PRC which does not exhibit significant dissipation after a certain sampling period. u_{max} can be used to estimate the minimal possible sampling rate for such compounds.

The variability of ke values can encompass about two orders of magnitude at high Koa levels and within one order of magnitude at lower K_{oa} values. Even after 1 year substantial dissipation for some high K_{oa} compounds could not be determined or is scattering around zero in relation to the analytical precision possible for active as well as passive sampling (Fig. 6). In contrast to other theories the measurements show that at low k_e-values the R_{vo} values are increasing dramatically and are indicating very high R_{vo} and thus very low concentrations in the free gas phase. Therefore it must be concluded that air concentrations estimated for PAH based on a similar VO design and the theories of Huckins et al. can be overestimated by orders of magnitude – especially if the sampling volume of a PRC with dissipation in the 80–20 % range is used to calculate gas-phase concentrations of compounds beyond 20 %.

Therefore an alternative method, based on the use of all in situ PRC data, including those whose PRC concentration remaining are close to the limit of detection LOD and those who's PRCs are non-depleted. To allow this approach, uncertainties are modelled using PRC data of field blanks never exposed to the environment. The Student-t distribution is used to obtain confidence limits for measurement uncertainty. Replicated VO-field blanks were measured to obtain a standard deviation that could be used directly as the standard analytical uncertainty. The uncertainty values were used to estimate the minimal sample rate R_{min}. Efforts to reduce bias and variability can be improved by increasing the number of blank samples. R_{min} was applied as the new values of PRC sampling rate $R_{vo,PRC}(N)$ if a direct measurement was not obtainable.

The VO-field blanks consisted of loaded samplers taken to and from the field with other VOs but never removed from their airtight vials. These blanks were prepared and analyzed simultaneously in the same manner as the deployed samplers to determine whether contamination or losses occurred during the VO loading, transport or analysis. A normal distribution for the results can be assumed, because the PRC concentrations can be well determined in cases of minor or no losses.

For each PRC, the standard deviation was calculated from obtained retained PRC values of the blank samples. The obtained values u_o of blank sample were first normalized in percentage $\%u$ according to the expected values u_w, following this equation (Fig. 6):

$$\%u = \frac{u_o}{u_w} \cdot 100 \qquad\qquad \text{Equation 32}$$

Then the standard deviation $Sn(\%)$ was obtained by following the equation:

$$Sn(\%) = \sqrt{\frac{\sum_{i=1}^{n} (\%u_i - \%\bar{u})^2}{n-1}} \qquad\qquad \text{Equation 33}$$

$\%u_i$, are the obtained values in percent for the blank sample i, $\overline{u}$ is the sample mean of the obtained values and n is the amount of blank samples used for the measurements.

The coefficient of variation CV (%) is calculated as following:

$$CV(\%) = \frac{S_n}{\%\overline{u}} \cdot 100 \qquad\qquad \text{Equation 34}$$

The standard error S_{CV} of the coefficient of variation is calculated as:

$$S_{CV} = \frac{CV}{\sqrt{2\,n}} \qquad\qquad \text{Equation 35}$$

The uncertainty (y) of the VO-field blanks is then:

$$y = CV + t_{a,v}S_{CV} \qquad\qquad \text{Equation 36}$$

Where $t_{a,v}$ is the critical value of Student's t for the chosen α level and for $v = n - 1$ degrees of freedom. The analysis is based on the best measurement capability. The uncertainty value ($y = CV - t_{a,v}S_{CV}$) is used to obtain the maximal retained PRC concentration after exposure time:

$$u_{max} = 100 - y, \qquad\qquad \text{Equation 37}$$

u_{max} is used to determinate the maximum possible elimination rate ke_{max} based on analytical uncertainty.

$$ke_{max} = -\frac{\ln(u_{max}/u_0)}{t} \qquad\qquad \text{Equation 38}$$

Thus the minimal expected sampling rate (Rs_{min}) is thereby deduced.

$$R_{vo_{min}} = V_{VO}K_{VO_a}ke_{max} \qquad\qquad \text{Equation 39}$$

$R_{vo_{min}}$ is used to adjust Rvo_{PRC} (Eq.1.3) to $R_{vo,PRC}(N)$. The *in situ* sampling rate of PRC $R_{vo,PRC}(N)$ represents the *in situ* sampling rate of target compound $R_{vo_{analyte}}$ *(N)* with similar physicochemical properties.

15.4 Chemicals sampled from the air compartment

PAH, PCB and OCP entering the natural ecosystems are distributed into the solid, liquid, or gaseous phases of environmental compartments. They release into the environment and stay persistent for many years because of their relatively low water solubilities and vapor pressures, and relatively large octanol-water and octanol-air partition coefficients. For instance, the spatial distribution of DDT and metabolites in Germany can clearly be attributed to historic application. Up to the 1980s, technical DDT was extensively used in the former Eastern Germany (GDR) and elevated concentrations are recently detected in wetland soil layers (Berger and Schwarzbauer, 2016). PAH are emitted into the atmosphere by various combustion sources including small wood stoves/boilers for domestic heating (Fernandes and Brooks, 2003; Bari et al., 2010) or released into the aquatic environment through the discharges from human activities such as industrial or domestic sewage effluents. In addition, it is well recognized that these contaminants are widely distributed all over the globe and atmospheric transport and temperature dependent partitioning between the atmosphere and environmental media is a leading pathway for their diffusion (Lohmann et al., 2007; Nizzetto et al., 2010). On the other hand, these persistent organic pollutants deposited in sinks such as water and ice are expected to revolatilize into the atmosphere, and there is evidence that this process may have already begun for volatile compounds (Ma et al., 2011).

Consequently, PAH, PCB and OCP may cause adverse human health effects even far away from their origin. In addition, it must be considered that the organisms may bioconcentrate low to relatively high levels of contaminants in their lipids. In the recent years, VO (Schramm et al., 2013) have been successfully used for determination of POPs in aquatic environment and sediments (Amdany et al., 2014; Temoka et al., 2016) due to their attractive qualities (i.e. their long-term stability, low cost, and ease of deployment). However, there are only limited published

data pertaining to the use of these passive sampling tools for the field of air monitoring. In this study, the level of PAH, PCB and OCP was determined in triolein containing VOs utilized as passive samplers for air and concentrations per cubic meter consisting of air + aerosols are estimated.

15.5 VO preparation

The procedure of VO sampler preparation in this study was similar to those described in Wang et al. 2009. In brief, low-density polyethylene lay flat tubing (LDPE, 2.5 cm wide, wall thickness 65 µm) supplied by VWR Ismaning, Germany was used. The LPDE tube was heat-sealed at a distance of 2.5 cm from one end. 700 µL of triolein (Sigma, Munich, Germany, 99 %) which was spiked with performance reference compounds (sixteen ^{13}C-EPA-PAH, ^{13}C PCB: PCB60, PCB127, PCB159) were added as close as possible to the sealed bottom by using a capillary pipette. The length of the whole VO was 29 cm and the triolein-containing part of the sampler (i. e., excluding the mounting loops) had an area of 115 cm^2. The sampler preparation was performed in a purified glovebox under nitrogen atmosphere to avoid contaminations. The prepared VO were stored in closely aluminium sealed heat cleaned 10 mL glass vials, further stored at –28 °C and kept cooled during transportation until deployment. The VO were transported in sealed flasks to and from the place of deployment. The VO were mounted in metal frames and placed in Stevenson screen boxes 2 m above the ground (Fig. 7). The VO were deployed at all the sampling sites from end of July 2015 till beginning of September 2015 for 43 days.

15.6 Sampling and locations

Three sampling locations at 270 m.a.s.l. (Bolzano city), 1700 m.a.s.l. (Ritten Station) and 2270 m.a.s.l. (the department for civil protection of Bolzano province, Rittner Horn) were arranged from the Italian Agency of Environment. In addition, a fourth sampling location was chosen in a private area of Mittelberg at 1100 m.a.s.l. (Pandelova et al. 2016)

Fig. 7: Picture of Stevenson hut and google map depicting the four locations of the altitude profile which was investigated in the framework of the Virtual Alpine Observatory (VAO)

15.7 Extraction, clean-up and analysis

The samples were spiked with a range of deuterated and ^{13}C-labeled compounds to monitor the extraction and cleanup procedures. VO were cut into small pieces and then extracted with 100 mL cyclohexane overnight at 200 rpm on a constant left-right shaker. The volume of generated extract for both sediment and VO samples was reduced to 1 mL and the residue was re-dissolved again with approximately 1–2 mL mixture of n-hexane:dichloromethane (1:1). Consequently, the sample underwent cleanup using a mixed column and C_{18} SPE cartridge (Wang et al., 2015). A recovery standard ([13]C_{12}-1,2,3,4-TCDD, Pentachlorotoluene, [13]C_{12}-1,2,3,7,8,9-HxCDD, PCB111) was added in the final eluate and the sample was concentrated with a gentle flow of nitrogen to 20 mL to be ready for analytical determination. The measurement was carried out with HRGC/HRMS. The parameters used for the isomer specific detection of PAH, PCB and OCP are given in (Temoka et al., 2016; Wang et al., 2015). All results were expressed on pg/VO, and those samples with contents less than the detection limit are reported as not detected (n.d.). The concentrations of the targeted analytes are then converted to concentrations per cubic meter air utilizing the PRC information to estimate the compound specific sampling rates of air.

15.8 Quality control/quality assurance

The accredited laboratory applies quality management system practices according to EN ISO/IEC 17025 standards. The applied analytical methods were regularly verified.

Laboratory blanks and field blanks were carried out. Laboratory blanks comprised the whole sample pre-treatment without VO in order to control the background levels of the studied compounds at the laboratory. All used solvents, silica, and alumina adsorbents were of trace analysis grade and supplied by LGC Standards (Wesel, Germany). The field VO blanks were carried to and from the place of deployment, and after being shortly opened at the deployment place, hermetically sealed again and then stored at –28 °C at the laboratory for the same period as the VO sampling deployment. The generated data was blank corrected by field blanks. Substances whose values after blank correction were lower than three times the standard deviation of the field blank value were considered as not detectable (n.d.) and the three times the standard deviation of the field blank value was provided in brackets. Analytes in samples that were not detected before field blank correction were given as not detectable (n.d.) with their limit of detection provided in brackets. The limit of detection of the instrumental methodology is considered as a signal/noise ratio 3:1. For VO samples, the recovery percentages for PCB, PAH, and OCP ranged from 40 % to 125 %.

15.9 Results of the altitude profile Bozen-Ritten

The PAH, PCB and OCP results (pg/m^{3}) in air (C_A) and air and aerosols (PM10) (C_{Total}) across the 4 sampling sides (270, 1100, 1700, and 2270 m.a.s.l.) are summarized in Table 1. Comparison of C_A and C_{Total} show that the portion of pollutant which can be attributed to the aerosol fraction is of minor relevance for those compounds which could be clearly identified and quantified in VO. The difference between C_A and C_{Total} increases only for compounds of very low vapor pressure such as 5-ring PAH, higher chlorinated PCB, and OCP of higher molecular weight eg. DDT. The main reason for this finding is the low concentration of aerosols in the remote alpine environment and proportions can be changed toward the aerosol fraction if the aerosol concentration increases substantially. The results show that the sampling of only aerosols is by far not sufficient to quantify the exposure of ambient air to living organisms.

Tab. 1: PAH, PCB and OCP results (pg/m^3) in air (C_A) and air and aerosols (PM10) (C_{Total}) across the 4 sampling sides (270, 1100, 1700, and 2270 m.a.s.l.)

	270 m.a.s.l.		1100 m.a.s.l.		1700 m.a.s.l.		2270 m.a.s.l.	
PM10 (µg/m^3)	14.4*		10**		9.7*		10**	
	C_A	C_{Total}	C_A	C_{Total}	C_A	C_{Total}	C_A	C_{Total}
PAH (ng/m^3)								
Naphthalene	29.55	29.55	n.d.	n.d.	n.d.	n.d.	n.d.	n.d.
Acenaphthylene	1.52	1.52	0.4566	0.4566	n.d.	n.d.	0.2808	0.2808
Acenaphthene	3.79	3.79	n.d.	n.d.	n.d.	n.d.	n.d.	n.d.
Fluorene	5.37	5.37	1.26	1.26	n.d.	n.d.	0.7145	0.7146
Phenanthrene	5.07	5.08	0.9635	0.9640	n.d.	n.d.	0.2886	0.2887
Anthracene	0.4318	0.4323	0.0446	0.0446	n.d.	n.d.	n.d.	n.d.
Fluoranthene	0.3461	0.3495	0.0527	0.0530	0.0087	0.0087	0.0120	0.0121
Pyrene	0.0392	0.0395	0.0031	0.0031	n.d.	n.d.	0.0020	0.0020
Benzo(a)anthracen	0.0003	0.0004	0.0001	0.0001	n.d.	n.d.	0.0001	0.0001
Chrysen	0.0010	0.0018	0.0001	0.0002	n.d.	n.d.	0.0001	0.0002
Benzo(b)fluoranthene	0.0027	0.0589	n.d.	n.d.	n.d.	n.d.	n.d.	n.d.
Benzo(k)fluoranthene	0.0092	0.2029	0.0032	0.0499	n.d.	n.d.	0.0022	0.0355
Benzo(a)pyrene	0.0032	0.0159	n.d.	n.d.	n.d.	n.d.	n.d.	n.d.
Indeno(1,2,3c,d)pyrene	n.d.	n.d.	n.d.	n.d.	n.d.	n.d.	n.d.	n.d.
Benzo(g,h,i)perylene	n.d.	n.d.	n.d.	n.d.	n.d.	n.d.	n.d.	n.d.
Dibenzo(a,h)anthracen	n.d.	n.d.	n.d.	n.d.	n.d.	n.d.	n.d.	n.d.
PCB (pg/m^3)								
PCB #28	38.21	38.35	21.69	21.75	21.29	21.35	23.91	23.97
PCB #52	17.34	17.47	8.22	8.26	8.00	8.04	7.12	7.16
PCB #101	10.85	11.24	3.12	3.20	3.23	3.31	3.18	3.26
PCB #138	1.16	1.34	n.d.	n.d.	n.d.	n.d.	0.4466	0.4963
PCB #153	1.68	1.96	n.d.	n.d.	n.d.	n.d.	n.d.	n.d.
PCB #180	0.0902	0.1492	n.d.	n.d.	n.d.	n.d.	0.0483	0.0703
PCB #77	0.4549	0.4746	n.d.	n.d.	0.2105	0.2166	0.1263	0.1301
PCB #81	n.d.	n.d.	n.d.	n.d.	n.d.	n.d.	n.d.	n.d.
PCB #126	0.0152	0.0194	n.d.	n.d.	n.d.	n.d.	n.d.	n.d.
PCB #169	n.d.	n.d.	n.d.	n.d.	n.d.	n.d.	n.d.	n.d.
PCB #105	0.8174	0.9431	0.1675	0.1854	n.d.	n.d.	0.1360	0.1505
PCB #114	0.1218	0.1370	0.0348	0.0379	0.0480	0.0520	0.0441	0.0479
PCB #118	2.01	2.21	0.4476	0.4799	0.3949	0.4225	0.3943	0.4228
PCB #123	n.d.	n.d.	n.d.	n.d.	0.0592	0.0629	0.0397	0.0422
PCB #156	0.0424	0.0716	n.d.	n.d.	n.d.	n.d.	0.0353	0.0521
PCB #157	0.0152	0.0264	n.d.	n.d.	n.d.	n.d.	0.0071	0.0107
PCB #167	0.0346	0.0473	n.d.	n.d.	n.d.	n.d.	0.0133	0.0167
PCB #189	0.0031	0.0129	n.d.	n.d.	n.d.	n.d.	0.0019	0.0061

15

	270 m.a.s.l.		1 100 m.a.s.l.		1 700 m.a.s.l.		2 270 m.a.s.l.	
	C_A	C_{Total}	C_A	C_{Total}	C_A	C_{Total}	C_A	C_{Total}
OCP (pg/m³)								
α-HCH	9.20	9.21	11.10	11.11	13.07	13.07	12.51	12.51
β-HCH	0.2240	0.2247	0.0907	0.0909	0.1182	0.1185	0.0659	0.0660
γ-HCH	38.03	38.15	9.61	9.63	9.34	9.36	9.36	9.38
δ-HCH	0.0755	0.0758	n.d.	n.d.	0.0499	0.0500	0.0546	0.0548
ε-HCH	n.d.	n.d.	n.d.	n.d.	n.d.	n.d.	n.d.	n.d.
Hexachlorobutadiene	n.d.	n.d.	n.d.	n.d.	n.d.	n.d.	n.d.	n.d.
Pentachlorobenzene	36.59	36.60	55.863	55.866	68.346	68.350	106.3	106.3
Hexachlorobenzene	143.1	143.1	209.2	209.3	321.2	321.2	412.0	412.1
Pentachloroanisole	135.8	136.0	104.1	104.3	108.2	108.3	145.9	146.1
Octachlorostyrene	0.5376	0.5634	0.7840	0.8101	0.7565	0.7809	1.42	1.46
4.4'-DDT	2.10	3.45	0.5697	0.8229	0.3949	0.5651	0.5524	0.7979
2.4'-DDT	0.97	1.46	0.3031	0.4088	0.2193	0.2935	0.3570	0.4816
4.4'-DDD	n.d.	n.d.	n.d.	n.d.	n.d.	n.d.	n.d.	n.d.
2.4'-DDD	n.d.	n.d.	n.d.	n.d.	n.d.	n.d.	n.d.	n.d.
4.4'-DDE	8.29	8.48	1.86	1.89	1.22	1.24	1.26	1.28
2.4'-DDE	0.2389	0.2449	0.0389	0.0396	0.0370	0.0376	0.0436	0.0444
trans-Chlordane	n.d.	n.d.	n.d.	n.d.	0.4221	0.4292	n.d.	n.d.
cis-Chlordane	1.46	1.51	0.9274	0.9484	0.7681	0.7850	n.d.	n.d.
oxy-Chlordane	n.d.	n.d.	0.6298	0.6709	0.6506	0.6917	0.8670	0.9235
Heptachlor	0.4101	0.4102	n.d.	n.d.	n.d.	n.d.	n.d.	n.d.
cis-Heptachloroepoxide	3.93	3.93	3.20	3.20	3.96	3.96	3.95	3.95
trans-Heptachloroepoxide	n.d.	n.d.	n.d.	n.d.	n.d.	n.d.	n.d.	n.d.
Aldrin	n.d.	n.d.	n.d.	n.d.	n.d.	n.d.	n.d.	n.d.
Dieldrin	3.40	3.42	2.07	2.08	2.31	2.32	3.17	3.18
Endrin	1.30	1.39	0.2868	0.2999	n.d.	n.d.	0.3151	0.3294
Endosulfan-I	3.97	4.01	3.03	3.05	2.64	2.6633	2.87	2.89
Endosulfan-II	0.2276	0.2276	0.1365	0.1365	0.0936	0.0936	0.0823	0.0823
Endosulfan-sulfate	0.3570	0.3801	0.2856	0.2985	0.3215	0.3356	0.2488	0.2601
Methoxychlor	n.d.	n.d.	n.d.	n.d.	n.d.	n.d.	0.3791	0.4208
Mirex	n.d.	n.d.	0.0222	0.0222	n.d.	n.d.	0.0381	0.0381
Cypermethrine	n.d.	n.d.	n.d.	n.d.	n.d.	n.d.	n.d.	n.d.

*   mean concentration during the sampling campaign measured on site.
** estimated concentration value

In practice the air concentration excl. particle contribution can be used to calculate the potential maximum concentration in the fat compartment (due to exposure to air without aerosols) of living organisms by using equation 18, 27 and 29 because the triolein is very similar to natural fat of organisms (data not shown). Values estimated like that can be also compared to existing limits for fatty feed and food.

15.10 Discussion

15.10.1 PAH distribution

A significant difference between the gas phase and the total concentration of gas and aerosol particle is not found in case of PAH of lower molecular weight. In general, the PAH concentrations decreased with altitude. No PAH except Fluoranthene were detectable at 1170 m.a.s.l. However, slight increase in concentrations was observed for the sampling location at 2270 m.a.s.l.

15.10.2 PCB distribution

Generally, the water solubility and volatility decrease as the degree of PCB chlorine substitution increases, and the lipid solubility increases with increasing chlorine substitution. Thus, PCB the levels in the aerosol compartment increased for higher chlorinated PCB. Regarding here investigated mountain profile a strong drop in PCB concentration was observed for the first three sampling sides. However, higher PCB concentrations were determined at Rittner Horn but the levels are far below those found in Bolzano city.

15.10.3 OCP distribution

Since the most OCP are volatile, these compounds are commonly found in the gas phase. Also, the difference between the total concentration (C_{Total}) and the gas phase (C_A) was in the range of 0–45 %. Some OCP compounds decrease with altitude, while other compounds increase (Pentachlorobenzene, Hexachlorobenzene and Octachlorostyrene).

4,4'-DDE and 4,4'-DDT are the major components of DDTs in all samples and the most abundant area with these compounds is determined in the valley of 270 m.a.s.l. Since the province of Bolzano is an industrial as well as wine production site the main source of DDT may come from historical uses.

15.11 Source apportionment

For the DDT group of chemicals the following ratios (Tab. 2) are proposed for judging about possible sources and/or the age of the contamination (Zhu et al., 2015).

Tab. 2: Ratios of DDT-compounds and their interpretation

(4,4'-DDE+4,4'-DDD)/4,4'DDT**<1**)	fresh 4,4'-DDT, resp. input
(4,4'DDE+4,4'DDD)/4,4'DDT**>1**)	aged 4,4'-DDT
(2,4'-DDE+2,4'-DDD)/2,4'DDT**<1**)	fresh 2,4' DDT, resp. input
(2,4'DDE+2,4'DDD)/2,4'DDT**>1**)	aged 2,4'-DDT
(4,4'DDE+4,4'DDD)/4,4'DDT **converging** (2,4'DDE+2,4'DDD)/2,4'DDT **dicofol** input	

In our study, the ratios are calculated for the altitude profile and compared to the actual concentrations found (Fig. 8).

For Bolzano profile the estimated ratio decreased with altitude and suggested fresher DDT input despite of decreasing DDTs-concentrations with altitude.

15.12 Conclusions

Ratios between chemical identities still indicate release of some OCP-POP and help for source apportionment of chemicals. Passive sampling employing VO is cheap and powerful for altitude

15
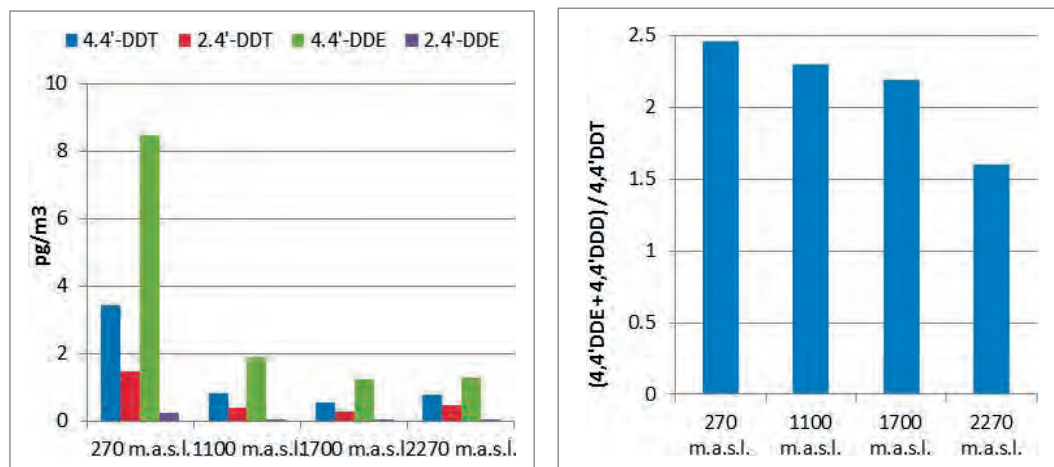
Fig. 8: Calculated (4,4'DDE +4,4'DDD)/4,4'DDT ratios (right) along Bolzano-Ritten altitude profile show that DDT is becoming 'fresher' with increasing altitude although the concentrations are decreasing with altitude (left)

profiling and indicative for long range transported POP. VO are suitable for the measurement of air quality of remote regions like the Alps with minor infrastructure. VO can also suit to estimate the exposure of the lipidome via air and compare the equilibrium concentrations of the natural fat like triolein to limits for fatty food and feed. Moreover it is possible to monitor also air and water in combination (Pandelova et.al. 2021) and conclude about the partitioning and exposomics of the chemicals between these two compartments.

Acknowledgments

References

Amdany, R., Chimuka, L., Cukrowska, E., Kukučka, P., Kohoutek, J. and Vrana, B. (2014) Investigating the temporal trends in PAH, PCB and OCP concentrations in Hartbeespoort Dam, South Africa, using semi-permeable membrane devices (VOs). Water SA. 40, 425–436.

Bari, M.A., Baumbach, G., Kuch, B., and Scheffknecht, G. (2010) Particle-phase concentrations of polycyclic aromatic hydrocarbons in ambient air of rural residential areas in southern Germany. Air Qual Atmos Health 3, 103–116.

Berger, M. and Schwarzbauer, J. (2016) Historical deposition of riverine contamination on terrestrial floodplains as revealed by organic indicators from an industrial point source. Water Air Soil Pollut 227: 20, 1–14.

Booij, K. and Smedes, F. (2010) An improved method for estimating in situ sampling rates of nonpolar passive samplers. Environ Sci Technol, 44, 6789–6794.

CDC 2010: http://www.cdc.gov/niosh/topics/exposome/

Chiou, C.T. (1985). Partition coefficients of organic compounds in lipid-water systems and correlations with fish bioconcentration factors. Environ Sci Technol 19, 57–62.

Fernandes, M. and Brooks, P. (2003) Characterization of carbonaceous combustion residues: II. Nonpolar organic compounds. Chemosphere 53, 447–458.

Huckins, J.N., Petty, J.D., Lebo, J.A., Almeida, F.V., Booij, K., Alvarez, D.A., Clark, R.C. and Mogensen, B.B. (2002). Development of the permeability/performance reference compound approach for in situ calibration of semipermeable membrane devices. Environ Sci Technol 36, 85–91.

Huckins, J.N., Petty, J.D., and Booij, K. (2006). Monitors of organic chemicals in the environment: Semi-permeable membrane devices. Springer, New York.

Lohmann, R., Breivik, K., Dachs, J., and Muir, D. (2007) Global fate of POPs: Current and future research directions. Environ Pollut 150, 150–165.

Ma, J., Hung, H., Tian, C., and Kallenborn, R. (2011). Revolatilization of persistent organic pollutants in the Arctic induced by climate change. Nature Climate Change 1, 255–260.

Mackay, D., Paterson, S. and Schroeder, W. H. (1986) Model Describing the Rates of Transfer Processes of Organic Chemicals Between Atmosphere and Water, Environ Sci Technol 20, 810–816.

Nizzetto, L., Lohmann, R., Gioia, R., Dachs, J., and Jones, K. (2010) Atlantic Ocean surface waters buffer declining atmospheric concentrations of persistent organic pollutants. Environ Sci Technol 44, 6978–6984.

Ockenden, W., Corrigan, B. Howsan, M. and Jones, K. (2001) Further developments in the use of semipermeable membrane devices as passive air samplers: Application to PCBs. Environ Sci Technol 35, 4536–4543.

Pandelova, M., Antritter, F., Feicht, E., Kirchner, M., Henkelmann, B., Corsten, C., Bernhöft, S., Verdi, L., Bachmann, C., Schramm, K.-W., 2016. Ambient air altitude profile of PAH, PCB and OCP near Bolzano determined by Virtual Organisms (VO). In: 36th Intl. Symposium on Halogenated Persistent Organic Pollutants http://www.dioxin20xx.org/index.html

Pandelova, M., Henkelmann, B., Lalah, J.O., Norf, H., Schramm, K.-W., 2021 Spatial, temporal, and inter-compartmental environmental monitoring of lipophilic pollutants by virtual organisms. Chemosphere 264, 128546

Schramm, K.-W., Wang, J., Bi, Y., Temoka, C., Pfister, G., Henkelmann, B. and Scherb, H. (2013) Chemical- and effect-oriented exposomics: Three Gorges Reservoir (TGR). Environ Sci Pollut Res 20, 7057–7062.

Söderström H S, Bergqvist P A. Passive air sampling using semipermeable membrane devices at different wind-speeds in situ calibrated by performance reference compounds. Environmental Science and Technology, 38: 4828–4834.

Temoka, C., Wang, J., Bi, Y., Deyerling, D., Pfister, G., Henkelmann, B. and Schramm, K.-W. (2016) Concentrations and mass fluxes estimation of organochlorine pesticides in Three Gorges Reservoir with virtual organisms using in situ PRC-based sampling rate. Chemosphere 144, 1521–1529.

Temoka, P., Pfister, G., Henkelmann, B., Schramm, K.-W. (2017) Adapting current model with field data of related performance reference compounds in passive samplers to accurately monitor hydrophobic organic compounds in aqueous media. Environ. Monit. Assess. 189:543

Wang, J., Bi, Y., Pfister, G., Henkelmann, B., Zhu, K., and Schramm, K.-W. (2009). Determination of PAH, PCB, and OCP in water from the Three Gorges Reservoir accumulated by semipermeable membrane devices (VO). Chemosphere 75, 1119–1127.

Wang, J., Liang, W., Henkelmann, B., Pfister, G., and Schramm, K.-W. (2015). Organochlorine pesticides accumulated by VO-based virtual organisms and feral fish in Three Gorges Reservoir, China. Environ Pollut 202, 160–167.

Zhu N., Schramm K.-W., Wang T., Henkelmann B., Fu J., Gao Y., Wang Y. and Jiang G. (2015). Lichen, moss and soil in resolving the occurrence of semi-volatile organic compounds on the southeastern Tibetan Plateau, China. Sci Total Environ, 518–519, 328–336.